JOURNAL OF COMPUTATIONAL PHYSICS 19, 29–42 (1975)

A Numerical Method for the Time-Dependent Krook Kinetic Equation

D. S. WATANABE

Department of Computer Science, University of Illinois, Urbana, Illinois 61801

Received July 31, 1974; revised April 9, 1975

Time-dependent problems in kinetic theory described by the Krook and other model kinetic equations can be formulated as systems of nonlinear Volterra integral equations. The derivation of these equations is described and a numerical procedure for solving them is presented. The nonlinear piston problem for the Krook equation is used to illustrate the discussion.

1. INTRODUCTION

Most nonlinear problems in kinetic theory can be treated only through approximation procedures of unknown accuracy. Krook [5, 6], however, has observed that the simplicity of the statistical model of molecular interactions renders many problems amenable to numerical treatment. His observation is valid for other models as well and provides an opportunity for evaluating the accuracy of approximation procedures through the comparison of approximate and exact numerical solutions.

One approach is the formulation of initial-boundary-value problems for model kinetic equations as systems of nonlinear integral equations for the basic moments. Steady problems give rise to Fredholm integral equations, while time-dependent problems give rise to Volterra integral equations. Although these equations are complicated and highly nonlinear, they can be solved with carefully constructed numerical methods.

Anderson [2, 3, 4] began a program to develop sophisticated numerical methods for solving a sequence of prototypical problems in kinetic theory. He developed methods for Fredholm equations which he used to solve several one-dimensional steady problems. Richter [9] extended the program to two-dimensional steady problems, and we extended it to time-dependent problems by developing numerical methods for Volterra equations. This paper describes how one of our methods can be applied to time-dependent problems in kinetic theory.

We first formulate the Volterra integral equations describing such problems. We then describe in general terms a general numerical procedure for solving these

equations and indicate how the various parts of the procedure can be tailored to accommodate particular problems. Finally, to illustrate our procedure, we examine the nonlinear piston problem for the Krook equation.

2. Integral Equation Formulation

Consider the general model kinetic equation

$$\partial f/\partial t + \mathbf{v} \cdot \partial f/\partial \mathbf{x} = \nu(\Phi - f). \tag{1}$$

The distribution function $f(\mathbf{v}, \mathbf{x}, t)$ is proportional to the probability density of molecular velocity $\mathbf{v} = (u, v, w)$ as a function of position $\mathbf{x} = (x, y, z)$ and time t. The convective rate of change of f, represented by the derivative on the left side of the equation, is balanced by the rate of change of f due to molecular interactions, represented by the model collision integral on the right. The function $\Phi(\mathbf{v}, \mathbf{x}, t)$ is a given function of a finite set of moments of f. Different model equations result for different choices of Φ. Thus the well-known Krook equation results if Φ is chosen to be the local isotropic Gaussian or Maxwellian distribution

$$F(n, \mathbf{q}, T) = n(2\pi T)^{-3/2} \exp(-(\mathbf{v} - \mathbf{q})^2/2T), \tag{2}$$

where the moments n, $\mathbf{q}$, and T are the local number density, flow velocity, and kinetic temperature, defined by the equations

$$\begin{aligned} n &= \int f \, d\mathbf{v}, \\ n\mathbf{q} &= \int \mathbf{v} f \, d\mathbf{v}, \\ 3nT + n\mathbf{q}^2 &= \int \mathbf{v}^2 f \, d\mathbf{v}. \end{aligned} \tag{3}$$

A more general model equation known as the ellipsoidal statistical model equation results if Φ is chosen to be an anisotropic Gaussian distribution. The collision frequency $\nu(\mathbf{x}, t)$ is a smooth positive functional of f. It is generally prescribed as a function of n and T in accordance with the law of force between molecules. We have assumed implicitly that the problem has been formulated in dimensionless form through a characteristic time $\bar{t}$, number density $\bar{n}$, and velocity $\bar{u}$, from which we derive a characteristic length $\bar{L} = \bar{u}\bar{t}$ and temperature $\bar{T} = m\bar{u}^2/k$, where m is the molecular mass and k is Boltzmann's constant.

We can transform the integrodifferential kinetic equation (1) into a pure integral equation by integrating along the characteristics of the convective differential operator. Consider an arbitrary point $\mathbf{x}$ in configuration space corresponding at

time t to a point within the gas. For an arbitrary point $\mathbf{v} \neq \mathbf{0}$ in velocity space, define a characteristic line through $\mathbf{x}$ with direction $\mathbf{v}$. A convenient parametric representation of this line is

$$\mathbf{y}(s) = \mathbf{x} - \mathbf{v}(t - s).$$

Along this characteristic, the kinetic equation may be written in the form

$$(d/ds) f(\mathbf{v}, \mathbf{y}, s) + \nu(\mathbf{y}, s) f(\mathbf{v}, \mathbf{y}, s) = \nu(\mathbf{y}, s) \Phi(\mathbf{v}, \mathbf{y}, s).$$

Let $\mathbf{x}_B$ be the first boundary point encountered on traversing the characteristic in the $-\mathbf{v}$ direction, and let t_B denote the corresponding value of the parameter s. If $t_B < 0$, set $t_B = 0$. The formal integration of the kinetic equation from t_B to t then yields

$$f(\mathbf{v}, \mathbf{x}, t) = f(\mathbf{v}, \mathbf{y}(t_B), t_B)\, e(t, t_B) + \int_{t_B}^{t} \nu(\mathbf{y}, s)\, \Phi(\mathbf{v}, \mathbf{y}, s)\, e(t, s)\, ds, \tag{4}$$

where

$$e(t, s) = \exp\left(-\int_{s}^{t} \nu(\mathbf{y}(s'), s')\, ds'\right), \tag{5}$$

and $f(\mathbf{v}, \mathbf{y}(t_B), t_B)$ is an initial or boundary distribution.

We assume that the gas is initially in equilibrium. Hence the initial distribution is the Maxwellian distribution

$$F(n_0, \mathbf{q}_0, T_0) = n_0(2\pi T_0)^{-3/2} \exp(-(\mathbf{v} - \mathbf{q}_0)^2/2T_0). \tag{6}$$

We further assume that molecules impinging on the boundary accommodate perfectly to the boundary velocity $\mathbf{q}_B$ and temperature T_B and subsequently are emitted according to the Maxwellian distribution

$$F(n_B, \mathbf{q}_B, T_B) = n_B(2\pi T_B)^{-3/2} \exp(-(\mathbf{v} - \mathbf{q}_B)^2/2T_B). \tag{7}$$

The pseudodensity n_B and temperature T_B are generally determined as part of the solution of the problem so as to assure zero net mass and energy flux normal to the boundary, that is,

$$\begin{aligned} \int \mathbf{n}_B \cdot (\mathbf{v} - \mathbf{q}_B) f(\mathbf{v}, \mathbf{x}_B, t)\, d\mathbf{v} &= 0, \\ \int \mathbf{n}_B \cdot (\mathbf{v} - \mathbf{q}_B)(\mathbf{v} - \mathbf{q}_B)^2 f(\mathbf{v}, \mathbf{x}_B, t)\, d\mathbf{v} &= 0, \end{aligned} \tag{8}$$

where $\mathbf{n}_B$ is the unit normal vector to the bounding surface at $\mathbf{x}_B$. The velocity $\mathbf{q}_B$ is usually specified but could be determined as part of the problem if equations describing the dynamic behavior of the boundary were prescribed.

Since ν, Φ, and the boundary distribution involve only a finite set of moments, the integral equation (4) reveals that the distribution function f is completely determined by these basic moments. Furthermore, we can use this equation to construct integral equations for these moments since they are defined in terms of f. These equations have the great advantage of depending on only four independent variables, $\mathbf{x}$ and t. For example, for the Krook equation we can construct a closed set of integral equations for n, $\mathbf{q}$, T, n_B, and T_B by setting Φ in Eq. (4) equal to the local Maxwellian distribution (2) and substituting the resulting expression into Eqs. (3) and (8). Once the solution of these equations has been found, the distribution function, if desired, can be obtained from Eq. (4) by quadrature.

The general form of these integral equations is illustrated by the equation for the moment,

$$m_{ijk}(\mathbf{x}, t) = \int u^i v^j w^k f(\mathbf{v}, \mathbf{x}, t)\, d\mathbf{v}.$$

It is simple to show that

$$\begin{aligned} m_{ijk}(\mathbf{x}, t) = &\int_{V_1} d\mathbf{v}\, u^i v^j w^k F(n_0, \mathbf{q}_0, T_0)\, e(t, 0) \\ &+ \int_{V_2} d\mathbf{v}\, u^i v^j w^k F(n_B, \mathbf{q}_B, T_B)\, e(t, t_B) \\ &+ \int_0^t ds \int_{V_3} d\mathbf{v}\, u^i v^j w^k \nu(\mathbf{y}, s)\, \Phi(\mathbf{v}, \mathbf{y}, s)\, e(t, s), \end{aligned} \tag{9}$$

where the V_i are appropriate subsets of velocity space. These integral equations are similar in form to the equations for steady problems, but their kernels are smooth, whereas the steady equation kernels contain logarithmic singularities [3] which arise because the steady convective operator vanishes when $\mathbf{v} = \mathbf{0}$. Due to their smooth kernels, the unsteady equations are in some respects easier to handle than their steady analogs.

3. Numerical Procedure

We have shown how initial-boundary-value problems can be formulated as systems of nonlinear Volterra integral equations. These equations are impervious to attack by analytical methods and must be solved numerically. We seek approximations to the solution on a discrete set of time mesh points $\mathscr{T} = \{t_i\}$, where $t_0 = 0$ and $t_{i+1} = t_i + \Delta t_i$ for $i \geqslant 0$. The problem is discretized by approximating the dependent variables at each t_i by an interpolation scheme involving a finite

number of free parameters and approximating the integral operators by a quadrature scheme. At each t_i the discretized equations are enforced on a set $\mathscr{X}$ of collocation points sufficient in number to determine the free parameters. The set of nonlinear transcendental equations obtained thereby can then be solved through an iteration scheme. In this way, the solution is computed step by step in time.

To devise an interpolation scheme, we must choose an appropriate space variable, deal if necessary with an unbounded domain, and select an efficient discrete representation. The choice of space variable depends on the structure of the solution and the geometry of the problem. For example, consider first a gas confined to a half-space bounded by an infinite flat plate initially at $x = 0$. The plate starts impulsively and thereafter moves with a constant velocity, producing a shock wave which moves away from the plate. The collisionless solution of this problem, valid for small times, is a function of the similarity space variable $\xi = x/t$. Hence it is computationally convenient to use the similarity variable for small times because it stretches and smooths the solution, making it numerically tractable. Consider next the flow generated by a circular cylinder of unit radius which starts impulsively and thereafter moves with a constant velocity. Given the problem geometry, it is natural to use polar coordinates (r, θ) fixed in the cylinder rather than Cartesian coordinates (x, y). For small times a similarity variable is again appropriate. However, for large times the variable $\rho = \arcsin(1/r)$ is useful because it can be shown that for sufficiently rarefied gases, the steady solution varies with r roughly as $\arcsin(1/r)$. This transformation has the additional advantage of mapping r into a finite interval. An even more powerful transformation can be obtained by applying an additional bilinear transformation to ρ. This provides additional flexibility in accommodating the structure of the solution. Note that we are not completely reformulating the problem in terms of new coordinates because this would introduce geometric pseudoforce terms and complicate the definition of characteristics.

We have seen how an appropriate transformation can be used to map an unbounded domain into a bounded one. An alternative procedure is to partition the unbounded domain into two sets: a finite set X on which the flow is not near equilibrium, and its complement $\bar{X}$. A discrete representation is used on X and an asymptotic representation is used on $\bar{X}$. In the first example cited above, the form of the solution for large x can be deduced analytically. It can be shown that the moment m_{ijk}, where j and k are even, decays as

$$m_{ijk}(\mathbf{x}, t) - m_{ijk}(\infty, t) \sim \alpha(x - v_s t)^{i/3} \exp(-\beta(x - v_s t)^{2/3}),$$

where v_s is the shock speed and α and β are certain constants. Note that this mode of decay is different from that predicted by continuum theory. Hence a "tail" of

this form can be fitted to the discrete representation, thereby yielding a representation over the entire domain.

Given a space variable and a finite domain of interpolation, we must still choose an efficient representation. The choice is conditioned by two conflicting criteria of efficiency. On the one hand, the number of free parameters in the representation must be minimized; on the other hand, an inexpensive process for evaluating the moments is essential. Splines satisfy both these criteria reasonably well, but their applicability is limited because the boundary values required for their specification are generally unavailable. However, splines can be used in problems where these values can be deduced from symmetries present in the problems. For example, splines in the angular variable θ can be used for exterior flows around cylinders. Another possible solution to this dilemma is the use of two representations: a primary representation adapted to the structure of the solution and selected for efficiency of sample utilization, and a secondary representation derived therefrom and selected for efficiency of evaluation. One useful primary representation is a finite Chebysev polynomial expansion. Its coefficients can be obtained from the well-known discrete orthogonality conditions under summation over certain sets of interpolation points. Chebysev expansions are particularly well suited for flows confined between two surfaces such as plane, cylindrical, and spherical couette flows because the sample points tend to cluster near the boundaries where they are best utilized. One possible secondary representation is a set of tables of the moments at equispaced sample points. Low-order Lagrange interpolation, centered if possible, can be applied to these tables to interpolate the solution in time and space at nonmesh points. The Lagrange rather than the difference or iterative form should be used because the Lagrange coefficients are identical for the different moments. Hence the relatively large amount of work required to evaluate the coefficients is spread over several variables, making the scheme efficient.

Three integral operators must be approximated: the time integration with respect to s, the velocity integration with respect to $\mathbf{v}$, and the time integration implicit in $e(t, s)$.

Although the moments vary smoothly in time, the time integrand can vary significantly over the subintervals $[t_i, t_{i+1}]$ particularly for small times. Hence standard interpolatory quadrature formulas employing the t_i as abscissas are generally inadequate. Instead, we approximate the time integration through a composite quadrature scheme employing the subintervals $[t_i, t_{i+1}]$. If the subintervals are of equal lengths, the Ralston composite formulas [8] are preferred because they are more accurate than the corresponding Newton–Cotes or Gaussian formulas. They are obtained by using Gaussian techniques in the interior of each subinterval and by requiring that the endpoints of each subinterval be abscissas with weights of equal magnitude but opposite sign. Hence when the formulas for each subinterval are summed, only the endpoints of the whole interval remain.

However, since the Δt_i may be unequal, we use low-order Gauss–Legendre formulas over each subinterval. Thus for example, if the n-point formula is used on each subinterval, the set $\mathscr{S}$ of s quadrature points for $t \in \mathscr{T}$ is

$$\mathscr{S}(t) = \{t_i + \theta_j \Delta t_i \mid t_i < t, 1 \leqslant j \leqslant n\},$$

where the θ_j are the Gauss–Legendre abscissas normalized to the interval [0, 1].

Although the moment equations involve three separate velocity integrations, the following remarks are applicable to all three. Each integration can be approximated in principle through a product quadrature scheme. The integrand in the u, v, and w integrations often is exponentially decaying. To adapt to this characteristic, each interval of integration should be divided into subintervals whose length is inversely proportional to the local variation of the integrand. However, this is difficult to do in a predetermined manner because the detailed structure of the integrand is difficult to ascertain. An adaptive quadrature scheme can be used to mimic this process. A simpler alternative is to divide the interval into equal subintervals whose length is a function of $\mathbf{x}$, t, and possibly s, chosen to resolve the integrand adequately. In some problems, this function can be determined empirically using the collisionless solution to determine the qualitative behavior of the integrand. Periodically during the actual integration, this function is examined and modified if necessary. Low-order Ralston or Gaussian quadrature formulas should be used on each subinterval to match the accuracy of the time quadrature. The set $\mathscr{V}$ of $\mathbf{v}$ quadrature points is the Cartesian product of the sets of u, v, and w quadrature points. Often the interval of integration is infinite. In such cases, we partition the interval into two sets: a set of v for which $\mathbf{y} \in X$, where the flow is not near equilibrium, and its complement for which $\mathbf{y} \in \overline{X}$. The composite rule is applied on the first set. On the second a Gaussian formula for semi-infinite intervals is used, or if the collision frequency ν is constant, the integrand is approximated using the equilibrium solution and the integral is evaluated analytically in terms of higher transcendental functions.

The most expensive quadrature is that in $e(t, s)$ because it lies at the heart of the computation. This quadrature must be performed at each time $t \in \mathscr{T}$, collocation point $\mathbf{x} \in \mathscr{X}$, time quadrature point $s \in \mathscr{S}$, and velocity quadrature point $\mathbf{v} \in \mathscr{V}$. Rather than perform the quadrature repeatedly, we instead compute a table of $\ln e(t, s)$ for an appropriate set of sample points in $\mathbf{x}$, s, and $\mathbf{v}$ and interpolate in this table to obtain the required values of $e(t, s)$. If the set of s sample points is chosen to be $\{s \mid s \in \mathscr{T}, s < t\}$, the composite time quadrature scheme described above can be used for the s' integration. Furthermore, additional interpolations of the moments in time are not required because the interpolants at the s' quadrature points are already required by the s integration from 0 to t.

The general form of the discretized equations is illustrated by the equation for $m_{ijk}(\mathbf{x}, t)$,

$$m_{ijk}(\mathbf{x}, t) = \sum_{\mathbf{v}\in\mathscr{V}_1(\mathbf{x},t)} w(\mathbf{v})\, u^i v^j w^k F(n_0, \mathbf{q}_0, T_0)\, e(t, 0)$$

$$+ \sum_{\mathbf{v}\in\mathscr{V}_2(\mathbf{x},t)} w(\mathbf{v})\, u^i v^j w^k F(n_B, \mathbf{q}_B, T_B)\, e(t, t_B)$$

$$+ \sum_{s\in\mathscr{S}(t)} w(s) \sum_{\mathbf{v}\in\mathscr{V}_3(\mathbf{x},t,s)} w(\mathbf{v})\, u^i v^j w^k \nu(\mathbf{y}, s)\, \Phi(\mathbf{v}, \mathbf{y}, s)\, e(t, s).$$

Here, $w(\mathbf{v})$ and $w(s)$ denote appropriate quadrature weights, the functions F, ν, Φ, and e denote appropriate interpolants, and the interpolants $e(t, s)$ are obtained from the tabular values

$$\ln e(t, s) = -\sum_{s'\in\mathscr{S}(t)-\mathscr{S}(s)} w(s')\, \nu(\mathbf{y}(s'), s').$$

The set of nonlinear transcendental equations obtained at each t_i by enforcing the discretized moment equations at the collocation points $\mathscr{X}$ has the form $\mathbf{m} = \mathbf{g}(\mathbf{m})$. This system of equations has several important properties. First, the number of unknowns is large. Second, all the unknowns are explicitly coupled and hence the system is dense. Third, although the interpolation scheme can be designed so that the moments sought at t_i are used in time interpolations only on the interval $[t_{i-1}, t_i]$, the iteration function $\mathbf{g}$ is still complicated and hence difficult and expensive to evaluate. Fourth, the general structure of the solution is known and is preserved by $\mathbf{g}$ in the neighborhood of the solution. The successive substitution iteration naturally suggests itself for this system. The iteration can be initiated using an approximation obtained by extrapolation from the solution at previous times. This simple iteration is useful only if it converges sufficiently rapidly. Fortunately this was the case in our calculations, but certain problems may require more sophisticated schemes. However, many well-known schemes for nonlinear systems cannot be used because of the properties of the system. For example, Newton's method is too expensive because of the density and complexity of the Jacobian. Anderson [1] has developed an extrapolation algorithm tailored to such systems. His algorithm is a generalization of false position and entails the linearization of the iteration function about several of the most recent iterates. The algorithm has been applied successfully to a variety of systems arising in the solution of nonlinear integral equations.

This procedure is not self-starting because the interpolation scheme involves the solution at several time steps. The required block of starting profiles can be

obtained simultaneously through Picard iteration. The quadratures are performed as outlined above, and the collisionless solution is used as the initial iterate. Once the starting values are obtained, the solution can be advanced step by step in time.

A rigorous error analysis of a procedure of this complexity would be extremely difficult and furthermore would yield an error bound so grossly pessimistic as to be worthless. We resort instead to an heuristic analysis which examines the self-consistency of the procedure under variation of the interpolation, quadrature, and iteration schemes. The variation of the numerical results under such perturbations provides heuristic estimates of the error. In addition the conservation laws and available limiting solutions provide certain algorithm-independent checks. Finally we can take some comfort in the knowledge that this procedure is modeled after a simpler one whose convergence has been rigorously established for a class of model problems [10].

4. Piston Problem

We have studied a variety of time-dependent problems using the integral equation approach. A simple illustration of our procedure is provided by the piston problem. Consider a monatomic gas with no internal degrees of freedom confined to a half-space bounded by an infinite flat plate. The plate, which is impermeable and insulated, starts impulsively from rest at time $t = 0$, when it is in the plane $x = 0$, and thereafter moves with constant velocity $\mathbf{i}$ into the gas. We regard the distribution function $f(\mathbf{v}, \mathbf{x}, t)$ as a function of x, but not of y and z, and assume that it is governed by the Krook kinetic equation. We further assume that the gas is initially at rest and in equilibrium with number density 1 and temperature T_∞, and that molecules impinging on the plate accommodate perfectly and subsequently are emitted with the Maxwellian distribution $F(n_B, \mathbf{i}, T_B)$.

We can derive the integral equations governing this problem using the procedure outlined above. These equations are complicated and their numerical solution is a formidable task. Since our interest is in exploring numerical techniques and not in solving this problem for a particular collision frequency model, we limit ourselves to the case where $\nu = 1$. The equations are considerably simplified in this case because the integration in $e(t, s)$ becomes trivial. This assumption does not mask any problems in our numerical procedure, however, because the integrand in $e(t, s)$ is well behaved in the general case and its numerical integration is straightforward. Our decision is prompted not by any pathology in the integration but only by its time-consuming nature.

Using the vectors

$$\mathbf{m} = \begin{bmatrix} n \\ nq \\ 3nT + nq^2 \end{bmatrix}, \qquad \mathbf{r}(u, T) = \begin{bmatrix} 1 \\ u \\ u^2 + 2T \end{bmatrix},$$

$$2\mathbf{d} = \begin{bmatrix} H_0(z) \\ (x/t)\, H_0(z) - (2T_\infty)^{1/2} H_1(z) \\ T_\infty[(3 + 2z^2)\, H_0(z) - 2zH_1(z)] \end{bmatrix}, \qquad \boldsymbol{\mu} = \begin{bmatrix} \alpha \\ \beta \end{bmatrix},$$

$$\boldsymbol{\rho}(u, T) = \begin{bmatrix} u - 1 \\ (u - 1)[(u - 1)^2 + 2T] \end{bmatrix}, \qquad 2\boldsymbol{\delta} = -(2T_\infty)^{1/2} \begin{bmatrix} H_1(z_B) \\ 2T_\infty[H_1(z_B) + H_3(z_B)] \end{bmatrix},$$

where q is the x component of $\mathbf{q}$ and

$$H_m(x) = 2\pi^{-1/2} \int_0^\infty y^m \exp[-(x - y)^2]\, dy,$$

$$z = x/t(2T_\infty)^{1/2}, \qquad z_B = (2T_\infty)^{-1/2},$$

$$\alpha = -n_B(T_B/2\pi)^{1/2}, \qquad \beta = 4\alpha T_B,$$

we can write the integral equations concisely as

$$e^t\mathbf{m}(x, t) = \mathbf{d}(x, t) + (2\pi)^{-1/2} \int_{x/t}^\infty du\, \mathbf{r}(u, T_B)\, n_B T_B^{-1/2} \exp[-(u - 1)^2/2T_B + s(u)]$$

$$+ (2\pi)^{-1/2} \int_0^t ds\, e^s \int_{-\infty}^{u(s)} du\, \mathbf{r}(u, T)\, nT^{-1/2} \exp[-(u - q)^2/2T], \qquad (10)$$

$$e^t\boldsymbol{\mu}(t) = \boldsymbol{\delta} + (2\pi)^{-1/2} \int_0^t ds\, e^s \int_{-\infty}^1 du\, \boldsymbol{\rho}(u, T)\, nT^{-1/2} \exp[-(u - q)^2/2T],$$

where

$$s(u) = -(x - ut)/(u - 1), \qquad u(s) = (x - s)/(t - s).$$

The problem so formulated is characterized by a single dimensionless parameter, the initial temperature T_∞.

We can use our numerical procedure to solve this sytem of equations. The similarity space variable $\xi = x/t$ is used, and for each t_i the interval $[1, \infty)$ is partitioned into two intervals: a finite interval X on which the moments are represented for simplicity by tables at equispaced sample points, and its complement $\bar{X}$ on which the moments are represented by asymptotic representations fitted to the tabular data. Periodically with increasing time, the length and mesh length of X are reduced to maintain a sufficient number of sample points within the developing wave. Lagrange interpolation, centered if possible, is used to interpolate the moments in time and space. The compromise velocity quadrature scheme is used rather than the adaptive scheme. Given the tabular interpolation

scheme, the interpolation sample points are the natural choice for the collocation points, and the system of nonlinear equations is solved by successive substitution.

The exact numerical solution for the initial temperature $T_\infty = 0.47407$ (shock Mach number 2) was computed for $t = 0(0.25)5, 5(0.5)10$. The parameters in the discretization scheme were chosen to assure self-consistency at a relative error level of 5×10^{-4}.

Figure 1 shows the number density, flow velocity, and kinetic temperature profiles for $t = 1, 2, 4, 6, 8$, and 10. The formation of a shock wave is evident. Note how the wave thickness increases linearly with time for small times. This property is the source of the effectiveness of the similarity space variable. If x were used, the mesh length would have to be extremely small initially and would have to be increased frequently to prevent the wasteful accumulation of sample points beyond the number necessary to resolve the wave. Moreover, the variation in time of the moments at a given point x would be large, making accurate interpolation in time difficult. However, with the similarity space variable, the wave thickness varies slowly, and the variation in time of the moments at a given point ξ is small. Hence the mesh length must be adjusted only occasionally, and accurate interpolation in time is easy.

The solution is in remarkable qualitative agreement with the linearized solution obtained analytically by Mason [7] for a specularly reflecting plate using the energy-conserving Krook model equation. The profiles are similar in form and

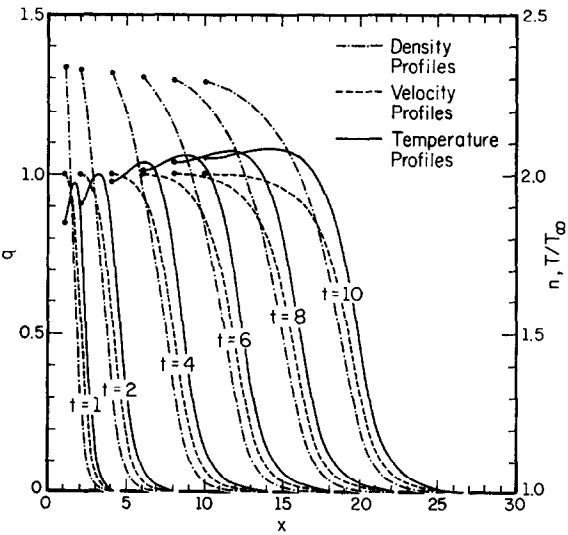

FIG. 1. Evolution of the number density, flow velocity, and kinetic temperature profiles for $T_\infty = 0.47407$ ($M = 2$).

evolve similarly in time, except at the plate because of the different boundary conditions. For example, in both solutions a temperature maximum is observed traveling (in a plate-centered coordinate system) first at the isothermal sound speed $T_\infty^{1/2}$ and then slowing to half the adiabatic sound speed $(5T_\infty/3)^{1/2}$ as the profile flattens. This agreement provides an independent check on the basic characteristics of the flow.

Figures 2–4 compare the developing number density, flow velocity, and kinetic temperature profiles with the exact steady Mach 2 profiles computed by Anderson [2]. The profiles are shown in a shock-centered coordinate system whose

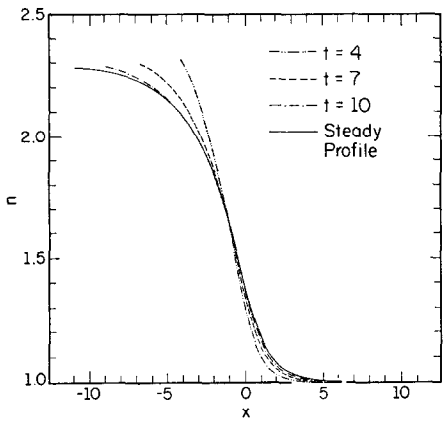

FIG. 2. Comparison of the steady and developing number density profiles for $T_\infty = 0.47407$ ($M = 2$).

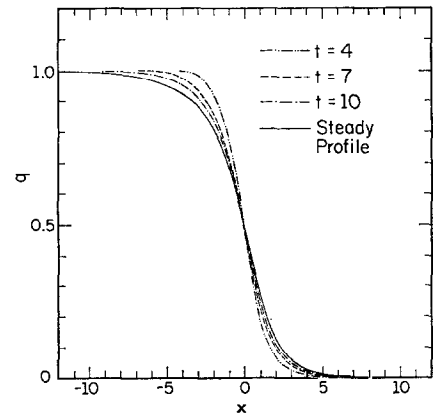

FIG. 3. Comparison of the steady and developing flow velocity profiles for $T_\infty = 0.47407$ ($M = 2$).

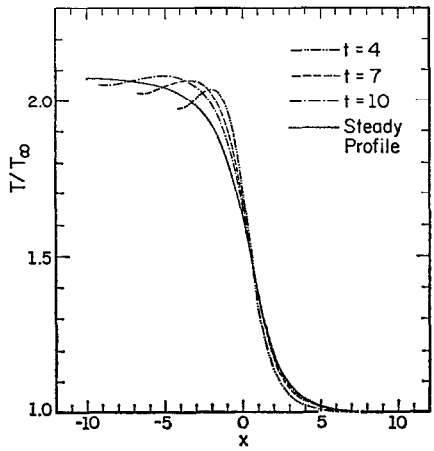

FIG. 4. Comparison of the steady and developing kinetic temperature profiles for $T_\infty = 0.47407$ ($M = 2$).

origin is chosen as the point where the flow velocity is equal to 0.5. As the initially steep gradients decrease with increasing time, the developing profiles approach the steady shock. This agreement provides an independent check on the accuracy of the solution.

The conservation of mass provides another independent check: the number of molecules displaced by the plate should equal the increase in the number of molecules in the disturbed region of the gas. Our solution satisfies this condition

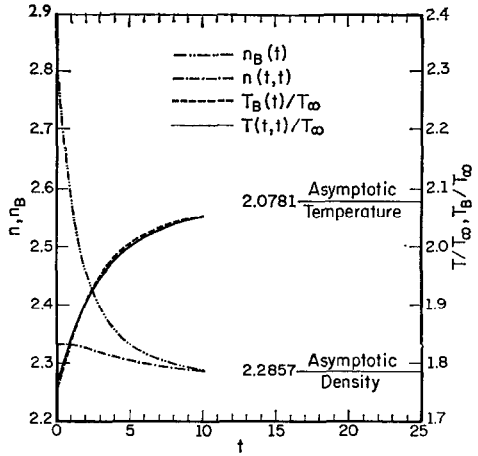

FIG. 5. Evolution of the number density and kinetic temperature at the plate for $T_\infty = 0.47407$ ($M = 2$).

with a relative error of 1×10^{-4}. Another such check is furnished by the asymptotic behavior of the number density and kinetic temperature at the plate. Figure 5 shows the evolution of these variables. Intuitively we expect $n_B(t)$ and $n(t, t)$ to converge and decrease to a common asymptotic number density. Similarly, we expect $T_B(t)$ and $T(t, t)$ to converge and increase to a common asymptotic temperature. The Rankine–Hugoniot conditions predict that the asymptotic number density and temperature are 2.2857 and 2.0781. The solution clearly fulfills our expectations.

5. Concluding Remarks

We have described how initial-boundary-value problems governed by model kinetic equations can be formulated as systems of nonlinear Volterra integral equations for the basic moments. We presented a numerical procedure for solving these equations and applied it to the nonlinear piston problem for the constant-collision-frequency Krook equation. Our procedure can be applied to problems for variable-collision-frequency models as well, but the appearance of nontrivial integrals of ν at the heart of the calculation leads to an order of magnitude increase in the computation time. Although this drastic increase can be reduced by efficient organization of the calculation, a more promising approach to such problems might be the computation of the distribution function through the direct integration of the kinetic equation with generalizations of finite difference methods for ordinary differential equations.

Acknowledgment

The author is grateful to Professor Donald G. M. Anderson for his helpful suggestions and advice. This work was supported in part by the National Science Foundation under Grants GK-65 and GK-1827.

References

1. D. G. Anderson, *J. Assoc. Comput. Mach.* **12** (1965), 547.
2. D. G. Anderson, *J. Fluid Mech.* **25** (1966), 271.
3. D. G. Anderson, *J. Fluid Mech.* **26** (1966), 17.
4. D. G. Anderson, *J. Plasma Phys.* **1** (1967), 255.
5. M. Krook, *Phys. Rev.* **99** (1955), 1896.
6. M. Krook, *J. Fluid Mech.* **6** (1959), 523.
7. R. J. Mason, *Phys. Fluids* **13** (1970), 1467.
8. A. Ralston, *J. Assoc. Comput. Mach.* **6** (1959), 384.
9. G. Richter, *Phys. Fluids* **16** (1973), 1599.
10. D. S. Watanabe, Ph.D. Thesis, Harvard University, 1970.